Precipitation in Northeast Mexico Primarily Controlled by the Relative Warming of Atlantic SSTs

Kevin T. Wright[1*], Kathleen R. Johnson[1], Tripti Bhattacharya[2], Gabriela Serrato Marks[3], David McGee[3], Dillon Elsbury[1,4,5], Yannick Peings[1], Jean-Louis Lacaille-Muzquiz[6], Gianna Lum[1], Laura Beramendi-Orosco[7], Gudrun Magnusdottir[8]

[1]Dept. of Earth System Science, University of California, Irvine; 3200 Croul Hall, Irvine, CA, USA.

[2]Department of Earth Sciences; Syracuse University, Syracuse, NY, USA.

[3]Department of Earth, Atmospheric and Planetary Sciences Massachusetts Institute of Technology; Cambridge, MA, USA.

[4]Cooperative Institute for Research in Environmental Sciences, Boulder, CO, USA.

[5]NOAA Chemical Sciences Laboratory, Boulder, CO, USA.

[6]Independent researcher; Ciudad Mante, Tamaulipas, Mexico.

[7]Instituto de Geología, Universidad Nacional Autónoma de México; Ciudad Universitaria, Ciudad de México, México.

Corresponding author: Kevin T. Wright (ktwright@uci.edu)

Key Points:

- We present the first speleothem record spanning the last millennium from NE Mexico using multiple geochemical proxies.
- In contrast to tree ring reconstructions, we suggest regional precipitation is primarily controlled by Atlantic SSTs.
- We utilize results from a forced-SST climate model to further support our interpretation.

Abstract

Reconstructing hydroclimate over the Common Era is essential for understanding the dominant mechanisms of precipitation change and improving climate model projections, which currently suggest Northeast Mexico will become drier in the future. Tree-ring reconstructions have suggested regional rainfall is primarily controlled by Pacific sea surface temperatures (SST). However, tree ring records tend to reflect winter-spring rainfall, and thus may not accurately record total annual precipitation. Using the first multiproxy speleothem record spanning the last millennium, combined with results from an atmospheric general circulation model, we demonstrate mean annual rainfall in Northeast Mexico is highly sensitive to Atlantic SST variability. Our findings suggest precipitation in Northeast Mexico may increase in the future in response to the relative warming of Tropical North Atlantic SSTs.

Plain Language Summary

We use geochemical markers of past rainfall in a cave stalagmite to show that variability in Atlantic sea surface temperatures strongly control the amount of precipitation in Northeast Mexico.

1 Introduction

Recent droughts in Mexico have led to significant economic crises, national food shortages and mass migrations, greatly impacting over 127 million people. Unfortunately, climate models suggest anthropogenic carbon emissions are likely to increase the frequency and intensity of droughts in the future. However, climate models poorly resolve detailed patterns of present and historic rainfall throughout most of Mexico and Central America, exhibiting particularly poor skill in modeling natural internal climate variability (Hidalgo et al., 2013). Additionally, a growing body of paleoclimate records from the Northern Tropics imply future droughts may not be as dire as model predictions, as the region may receive increased precipitation in response to a warmer climate (He & Soden, 2017; Sachs et al., 2009), though it is unclear if increased precipitation will extend to Northern Mexico. Paleoclimate constraints on the response of regional precipitation to internal climate variability and external forcing is of utmost importance for evaluating climate models and mitigating the impacts of future rainfall change, yet few records exist in Northern Mexico.

Tree ring records based on classical dendroclimatology (tree ring width) suggest interannual to multidecadal hydroclimate variability in Mexico is dominated by changes in Eastern Equatorial Pacific (EEP) SSTs, dominantly associated with the El Niño Southern Oscillation (ENSO) and to a lesser magnitude, the lower frequency Pacific Decadal Oscillation (PDO). Warm EEP SSTs are thought to drive a dipole precipitation pattern, with wet conditions in Northern Mexico and dry conditions in Southern Mexico. While drying in Southern Mexico in response to warmer EEP SSTs has been confirmed with paleoclimate records and modeling studies (Bhattacharya & Coats, 2020), increased precipitation in Northeast Mexico remains poorly constrained, with weaker than expected or inconsistent correlations in instrumental records, classical tree ring data, and tree ring isotopic data (Gutiérrez-García et al., 2020; Stahle et al., 2016; Villanueva-Diaz et al., 2007). Surprisingly, the role of SSTs in the Tropical North Atlantic, the dominant source of moisture for Mexico, remains enigmatic and could obscure the effect of Pacific SSTs. For instance, a positive phase of the Atlantic Multidecadal Variability (AMV) has been invoked to

explain broad drying in Northeast Mexico (Stahle et al., 2016) but instrumental data (Curtis, 2008) and tree ring records from nearby Texas (Gray et al., 2004), as well as records of runoff on interannual to orbital scales from Northeast and Central Mexico (Roy et al., 2016, 2020; Wogau et al., 2019), suggest warmer Atlantic SSTs may drive the opposite response, with regional increases in precipitation. Speleothem records from Northern Mexico covering the more recent past (Common Era) can provide a robust record of past hydroclimate variability to help clarify the role of Atlantic versus Pacific SSTs on regional precipitation, but none exist in the region.

To address this gap, we have developed the first continuous inter-annually resolved stalagmite record (CB4) of hydroclimate covering the last millennium utilizing four geochemical proxies: stable oxygen isotopes ($\delta^{18}O$), carbon isotopes ($\delta^{13}C$), trace elements (Mg/Ca), and dead carbon proportion (DCP, ^{14}C). The sample was retrieved from Cueva Bonita (23°N, 99°W; 1071 m above sea level) located in the northern-most tropical rainforest on the windward side of the Sierra Madre Oriental in the Northeast state of Tamaulipas (Figure 1, Figure S1, supplementary materials). The stalagmite age model is constrained by 19 U-Th dates and fluorescent layer counting (Figure S2), and extends from 833 CE to 2017 CE, when the sample was collected (supplementary materials). Previous research has often interpreted $\delta^{18}O$ as a proxy for weighted mean annual precipitation amount (Baker et al., 2020), which we also demonstrate is the predominant influence on $\delta^{18}O$ at Cueva Bonita (Figure S3). However, a growing number of studies have shown that $\delta^{13}C$, Mg/Ca, and dead carbon proportion (DCP) are also potentially reliable proxies for local water balance (Michael L. Griffiths et al., 2020), improving our interpretation of hydroclimate when combined with speleothem $\delta^{18}O$ (see supplementary text).

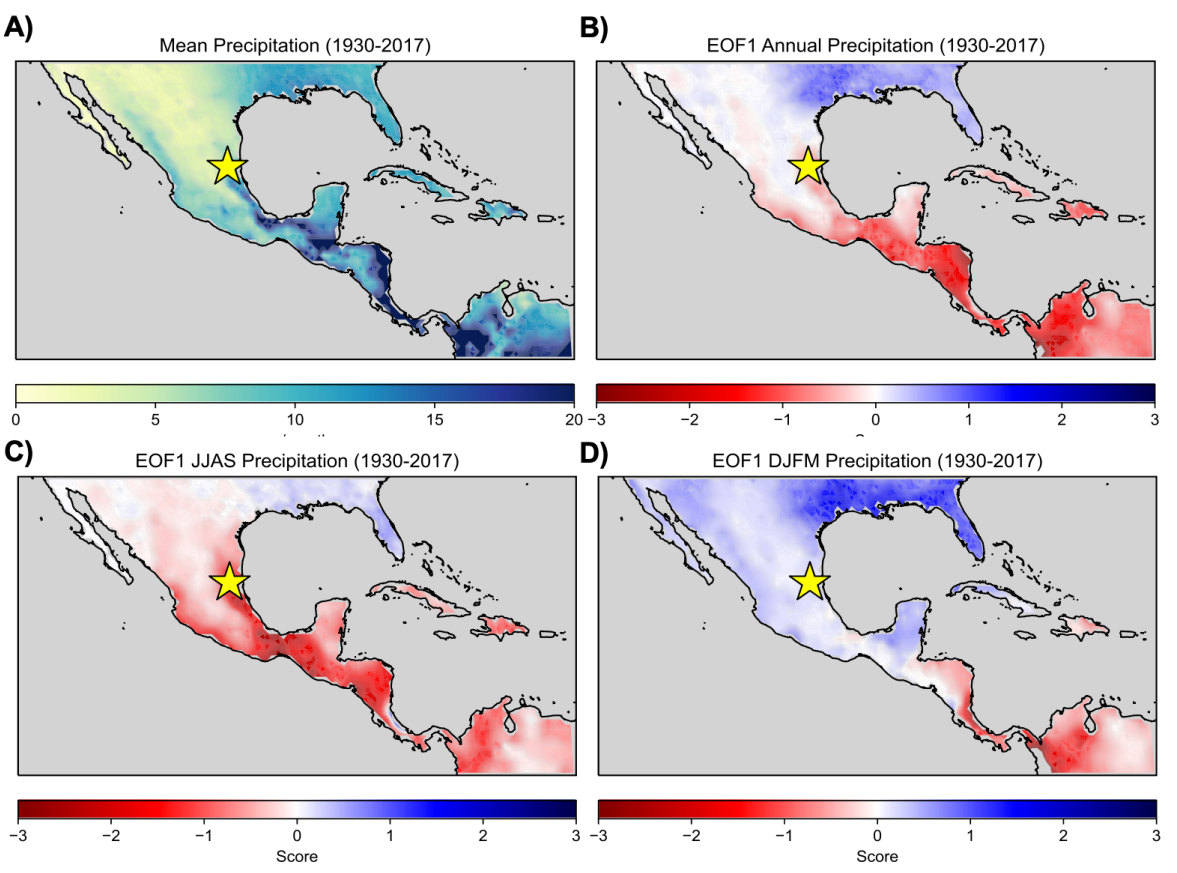

Figure 1. Precipitation patterns in Mexico. a) Mean precipitation over Mexico, Central America, and the Circum-Caribbean region**. b)** EOF1 of mean annual precipitation. **c)** EOF1 of mean summer (JJAS) precipitation. **d)** EOF1 of mean winter (DJFM) precipitation.

2 Data and Methods

2.1 Chronology

The CB4 stalagmite was cut, polished and sampled for 15 U-Th dates along its vertical growth axis using a Dremel hand drill with a diamond dental bur. The CB4 sample has uranium concentrations ranging from 37 to 160 ng/g (Table S1). Calcite powder samples weighing 250-300 mg were prepared at Massachusetts Institute of Technology following methods similar to Edwards et al., (1987) (Lawrence Edwards et al., 1987). Powders were dissolved in nitric acid and spiked with a $^{229}Th - ^{233}U - ^{236}U$ tracer, followed by isolation of U and Th by iron co-precipitation and elution in columns with AG1-X8 resin. The isolated U and Th fractions were analyzed using a Nu Plasma II-ES multi-collector inductively coupled plasma mass spectrometer (MC-ICP-MS) equipped with an Aridus 2 desolvating nebulizer, following methods described in Burns et al. (2016) (Burns et al., 2016). The corrected ages were calculated using an initial $^{230}Th/^{232}Th$ value of 9.8 ± 4.9 ppm to correct for detrital ^{230}Th. The 9.8 ppm initial Th correction value was determined by testing dates corrected with different initial ^{230}Th corrections for stratigraphic order following methods laid out by Hellstrom et al. (2006) and matching the ages with the radiocarbon bomb peak depth. The uncertainty of 4.9 ppm was scaled proportionally to the normal ± 50% correction (4.4 ± 2.2 ppm). U-Th ages range from 78 ± 96 to 2119 ± 162 years before present, however, this study focused on the top 100mm of the sample with an oldest date of 1189 ± 154 (where present is 1950 CE). All 15 dates fall in stratigraphic order within 2σ uncertainty (Table S1), but two were identified to be outliers based on low probability of fit for age models (Figure S2). U-Th ages were combined with fluorescent layer counting to decrease uncertainty. The 95% confidence interval for the age-depth model was constructed using 2000 Monte-Carlo simulations through the age-depth modeling software COPRA (Breitenbach et al., 2012).

2.2 Stable Isotope and Trace Element Analysis

CB4 was micro-sampled for both stable isotope and trace element analyses using a Sherline micromill at 250 μm increments to a depth of 1 mm, producing 400 samples. The powder for CB4 was collected, weighed out to 40 - 80 μg and analyzed on a Kiel IV Carbonate Preparation Device coupled to a Thermo Scientific Delta V-IRMS at the UC Irvine Center for Isotope Tracers in Earth Sciences (CITIES) following methods described by McCabe-Glynn et al. (2013) to determine $\delta^{18}O$ and $\delta^{13}C$ (McCabe-Glynn et al., 2013). Every 32 samples of unknown composition were analyzed with 14 standards which included a mix of NBS-18, IAEA-CO-1, and an in-house standard. The analytical precision for $\delta^{18}O$ and $\delta^{13}C$ is 0.08‰ and 0.05‰, respectively.

For trace element analysis, 20 - 60 μg calcite powder samples were dissolved in 500 μL of a double distilled 2% nitric acid solution. The samples were analyzed using a Nu Instruments Attom High Resolution Inductively Coupled Plasma Mass Spectrometer (HR-ICP-MS) at the CITIES laboratory. Mg/Ca ratios were calculated from the intensity ratios using a bracketing technique with five standards of known concentration and an internal standard (Ge) added to all

samples to correct for instrumental drift. Trace element analysis of CB4 serves to complement the interpretation of speleothem $\delta^{18}O$ and $\delta^{13}C$; therefore, a lower-resolution (multi-decadal to centennial) analysis was conducted over the complete record by analyzing every other sample (200 total; Table S3). For plotting/aesthetic purposes, CB2 Mg/Ca, $\delta^{18}O$ and $\delta^{13}C$ were smoothed using a moving average. The pandas function DataFrame.rolling().mean()was utilized to smooth the data for plotting only, with the size of the moving window set to 4. The full data set reported in the supplementary materials is unsmoothed.

2.3 Forced SST Model Simulations

We use the specified chemistry version of the Whole Atmosphere Community Climate Model (SC-WACCM4) with Community Atmosphere Model version 4 (CAM4) physics (Marsh et al., 2013; Smith et al., 2015). The model domain extends from the surface up to 145 kilometers over 66 vertical levels with a horizontal resolution of 1.9 by 2.5 degrees latitude and longitude. The control simulation is a 200-year continuous integration of the model that is forced with a fixed repeating annual cycle of present-day SST/sea ice concentration variability (1979–2008 average annual cycle from the Hadley Centre Sea Ice and Sea Surface Temperature dataset (HadISST) (Rayner et al., 2003). Forced SST simulations are identical to the control, except that forced SST anomalies corresponding to the cooling/warming of the Atlantic and/or Pacific are superimposed on top of the control run SST. The prescribed SST patterns of cooling/warming correspond to the Atlantic Multidecadal Variability (AMV) and the Interdecadal Pacific Variability (IPV) SST patterns, as derived from observations. These perturbation simulations are also run for 200 years. Taking the difference between the atmospheric fields in these perturbation simulations and that in the control allows us to cleanly isolate the atmospheric response to SST anomalies from internal variability.

2.4 Radiocarbon Laboratory Methods

Calcite samples were analyzed for ^{14}C at University of California, Irvine within the Keck Carbon Cycle Accelerator Mass Spectrometry (KCCAMS) laboratory. Calcite powders were leached with 10% HCl acid, to remove any secondary carbonates, and hydrolyzed with 85% phosphoric acid. Using a modified hydrogen-reduction method (Beverly et al., 2010), samples were then graphitized onto a Fe catalyst. During data processing calcite powder from a radiocarbon free speleothem was used for blank subtraction.

3 Results and Discussion

3.1 Warmer Atlantic SSTs Drive Extended Wet Periods in NE Mexico

The most striking centennial-scale feature of this record is the extremely low speleothem $\delta^{18}O$ values of -6.5‰ at ~1490 CE (Figure 2), which is also supported by very low $\delta^{13}C$ values (-11‰) and Mg/Ca ratios (38 mmol/mol) near the same time. Increased precipitation during the 15th century has been suggested as a dominant driver of population expansion at major archaeological sites, including Tenochtitlan in the Basin of Mexico, and has thus been referred to as the Aztec Pluvial (Sanders et al., 1979). Stahle et al. (2016) provided evidence that the Aztec Pluvial could be a major wet period over the Common Era, but lacked older tree ring records to confirm the magnitude and spatial extent of increased precipitation. Our record confirms through

multiple geochemical proxies that the Aztec Pluvial represented the wettest conditions in Northeast Mexico over the last millennium. Speleothem $\delta^{18}O$ from Juxtlahuaca cave in SW Mexico and Ti concentration in lake sediments from Central Mexico also show increased precipitation during this interval (Lachniet et al., 2017; Wogau et al., 2019), suggesting the Aztec Pluvial impacted at least Northeast, Central and Southwest Mexico, if not the entire country. While a strengthening of the North American Monsoon has been invoked to explain increased precipitation in Southwest and Central Mexico (Lachniet et al., 2017), NE Mexico is outside the monsoon's dominant core region and we therefore suggest this mechanism is not likely to increase precipitation in this region. A comparison of Cueva Bonita $\delta^{18}O$ to Eastern and Tropical North Atlantic SSTs instead suggests the 15th century pluvial period was likely forced by anomalously warm Atlantic SSTs (Figure S4-5). Warmer SSTs increase precipitation in NE Mexico by increasing boundary layer moisture convergence, as well as favoring the development of hurricanes (Wang & Lee, 2007).

Notably, the CB4 record also indicates a pattern of decreasing $\delta^{18}O$ values (from -3.5‰ to -6.7‰) beginning near the start of the pre-industrial period, around 1830. This trend is also supported by a shift towards more negative $\delta^{13}C$ values (-8.9‰ to -13‰) and decreased Mg/Ca ratios (54 to 28 mmol/mol), suggesting an increase in both regional and localized precipitation with anthropogenic warming. The decreasing trend of $\delta^{18}O$ and $\delta^{13}C$ appears to be in response to Atlantic warming, as Pacific warming is delayed until the early- to mid-20th century (Figure S5). Interestingly, this trend towards wetter conditions is not obvious in Mexican tree rings (Stahle et al., 2016), but is evident in historical precipitation records, satellite data and re-analysis data from Central Mexico (Martinez-Lopez et al., 2018), suggesting precipitation increases may occur only in summer and early autumn. Although our

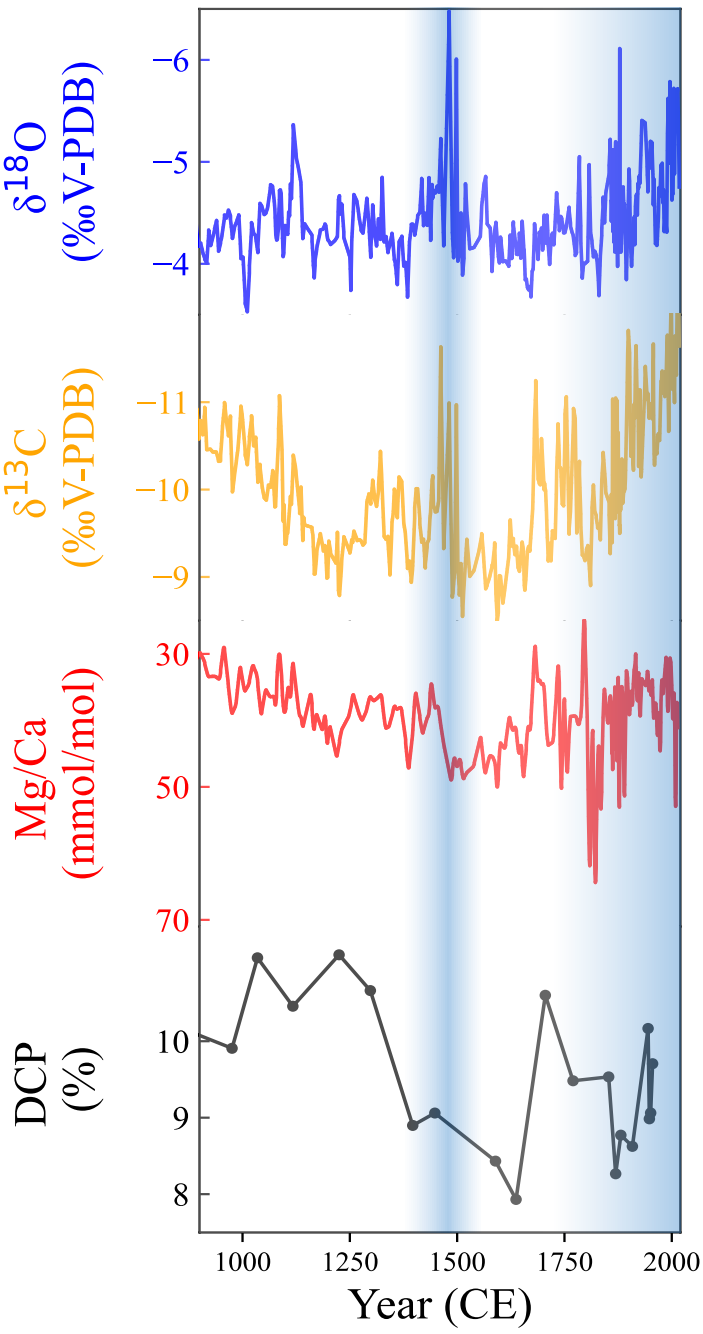

Figure 2. Results of CB4 geochemical proxies. Speleothem $\delta^{18}O$, $\delta^{13}C$, Mg/Ca ratios and DCP over the last millennium. Speleothem $\delta^{18}O$ and $\delta^{13}C$ have an average resolution of 3 years, Mg/Ca ratios have an average resolution of 6 years, and DCP has an 83 year average. Results of CB4 proxies show a similar response on multi-decadal to centennial timescales. Compared to $\delta^{18}O$, proxies show a moderate to strong correlation on multidecadal timescales ($\delta^{13}C$ $r = 0.56$, $p < 0.05$; Mg/Ca $r = 0.29$, $p < 0.05$). Shading in blue represents wet periods during the Aztec Pluvial at ~1450, and during the industrial period (~1800-2017).

record does not possess sub-annual resolution to verify, we suggest the wetting trend may be driven by more extreme pluvial climate events in the late-summer and early-autumn months, such as tropical storms and hurricanes, that are becoming both more frequent (Bhatia et al., 2019) and decaying more slowly on land (Li & Chakraborty, 2020) under current anthropogenic climate change.

3.2 The role of Pacific and Atlantic SSTs on Multidecadal Variability

The strong positive correlation of NE Mexico rainfall to Atlantic SSTs is surprising, considering tree ring records have provided robust evidence of spatially widespread drying in response to positive phases of the AMV (Stahle et al., 2016). However, our record demonstrates a strong positive correlation to Atlantic SSTs not only on centennial timescales but on multidecadal timescales as well. This is evident in a direct comparison of proxies over the last ~800 years (Figure S4-5), wavelet power spectrum analysis demonstrating a periodicity of 66 years for $\delta^{18}O$ and 55 years for $\delta^{13}C$ (Figure S6), which is close to the previously suggested periodicity of 65 years for the AMV (Schlesinger & Ramankutty, 1994), and a direct comparison of the AMV index to CB4 $\delta^{18}O$ over the last century (Figure 3a). Previous reconstructions of runoff in NE Mexico speculated the AMV likely altered regional hydroclimate in the early Holocene and Late-Pleistocene (Roy et al., 2016), but did not retain the temporal resolution required to verify. Our record provides the first multiproxy evidence of AMV influence on NE Mexico precipitation over the last millennium.

Interestingly, CB4 proxies not only contrast tree ring interpretations of the role of Atlantic SSTs, but speleothem $\delta^{18}O$, $\delta^{13}C$, and Mg/Ca ratios also record wetter conditions during periods of cool Eastern Pacific SSTs, a response also reflected in additional speleothem records from Southern Mexico and Central America (Lachniet et al., 2004, 2017). The similarity in speleothem records across both Northern and Southern Mexico suggests precipitation may not be out-of-phase in these two regions as previously thought. Modern instrumental data also suggests precipitation is mostly in-phase during seasonal (summer) and annual timescales (Figure 1), only showing a strong dipole precipitation pattern for winter rainfall (Figure 1, supplementary material). While changes in winter-spring soil moisture, as typically recorded by tree ring chronologies, are closely linked to changes in early summer soil moisture, they can be poorly correlated with late summer and autumn rainfall (St. George et al., 2010; Stahle et al., 2016). We therefore suggest the discrepancies between the speleothem data presented here and previous tree ring-based interpretations are potentially driven by the seasonal bias of tree rings to record winter-spring and early summer precipitation. While analysis of instrumental data supports this notion, with a positive phase of the AMV leading to increased precipitation in NE Mexico (Figure 3b), historical rainfall is complicated as it is also impacted by Pacific variability and the complex interactions between variability in the Atlantic on the Pacific, and vice versa (Bhattacharya & Coats, 2020).

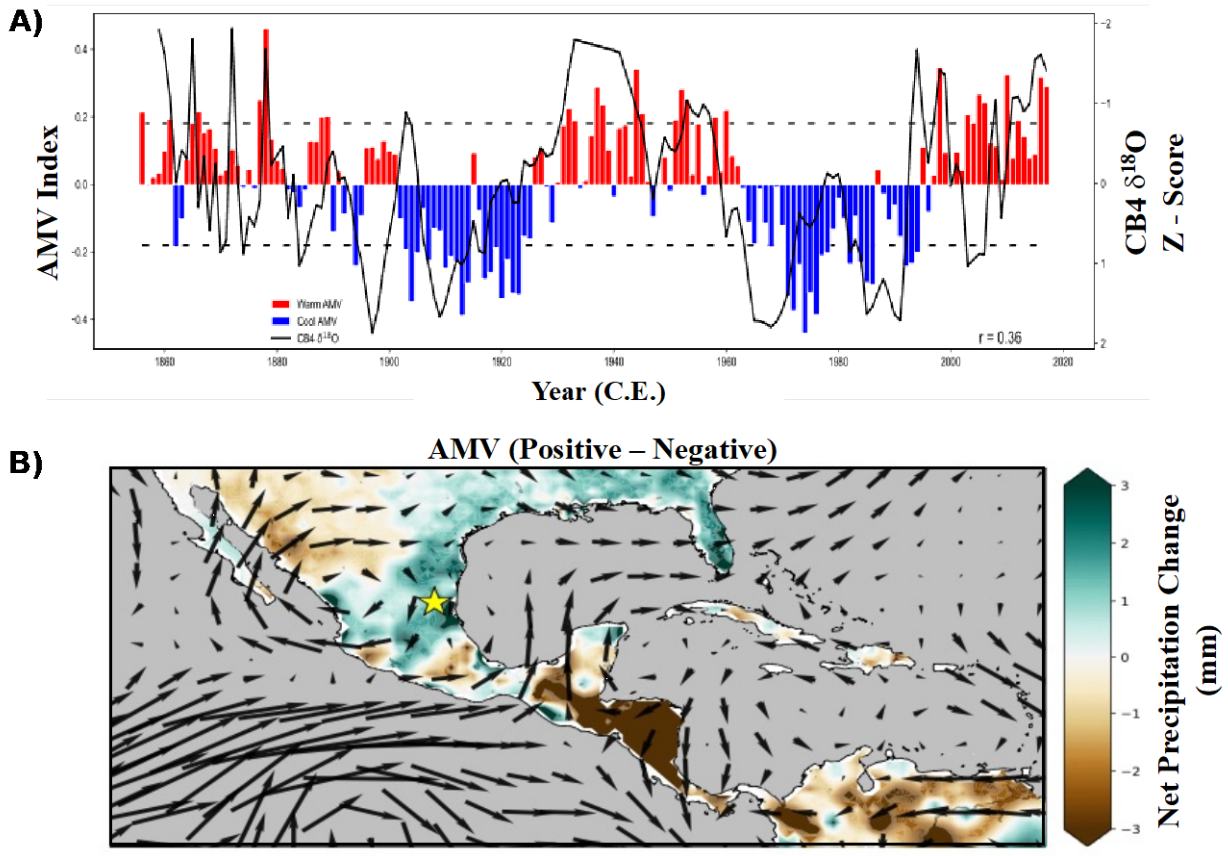

Figure 3. Comparison of AMV to CB4, precipitation and low-level winds. a) Both records are detrended to account for the impact of anthropogenic warming on Atlantic SSTs. The $\delta^{18}O$ appears to correspond strongly to the AMV Index over the last ~150 years, capturing both extended periods of positive phases (1920-1960, 2000-2020+) and extended negative phases (1900-1920, 1960-2000). Surprisingly, CB4 even captures some the short-term variability (1860-1900). **b)** Comparison of AMV phases (positive minus negative) on mean low-level winds and precipitation. A positive phase leads to increased precipitation in NE Mexico, but drying in NW and Southern Mexico.

3.3 Forced SST Model Simulations and Mechanisms of Precipitation Change

To test the seasonality and spatial pattern of rainfall in response to SST variability, we utilized a state-of-the-art general circulation model with prescribed patterns of Atlantic and Pacific SST variability. This experimental design allows us to disentangle the influence of the Pacific variability on the Atlantic, and vice-versa. Control runs of this model reliably capture global patterns of observational precipitation and low-level winds (Smith et al., 2015), including Mexico and Central America (Figure S7-8). While our analysis includes a full range of forced-SST conditions, the natural environment on interannual to decadal timescales is most likely to exhibit an Atlantic-Pacific out-of-phase warming or cooling via changes in the strength of the Walker Circulation (Fosu et al., 2020), and are therefore the focus of this discussion.

During summer, in response to a warm Pacific and cold Atlantic, precipitation decreases across almost all of Mexico and Central America (Figure 4). Anomalous convection in the Pacific in response to warmer conditions has previously been attributed to drying via an enhanced Walker Circulation, which is also simulated in this study (Figure S9-10). This results in a southward migration of the Atlantic ITCZ and stronger easterly trade winds (Bhattacharya et al., 2017; Bhattacharya & Coats, 2020; Chiang & Sobel, 2002; Giannini et al., 2000, 2001). While the contraction of the ITCZ is known to decrease precipitation in Southern Mexico and Central America (Asmerom et al., 2020), stronger easterly trade winds are thought to increase precipitation in Northern Mexico via an intensification of easterlies and the Caribbean Low-Level Jet (CLLJ) (Wang & Lee, 2007). Although low-level wind anomalies in model simulations correctly replicate the intensification of the CLLJ (Figure 4), models demonstrate this instead leads to decreased precipitation over much of Mexico. This response is also replicated when SST conditions are reversed, which drives a weakening of the CLLJ and increased precipitation. While on longer, orbital to interannual timescales, a stronger CLLJ has been attributed to drier conditions in NE Mexico by cooling Atlantic SSTs via an enhanced wind-evaporation-SST feedback loop (Wright et al., 2021), this experiment utilizes prescribed SSTs and we therefore cannot attribute observed precipitation changes to this mechanism. We instead suggest that warmer Atlantic SSTs lead to a reduction in the strength of the CLLJ and, consequently, vertical wind shear. Decreased vertical wind shear appears to be further amplified by cooler Pacific SSTs (Figure S12-13), which fosters the formation of deep convective storms and increases precipitation throughout most of Mexico (Figure 4). This mechanism is further supported by observational records and previous modelling results (Wang, 2007; Wang & Lee, 2007), which

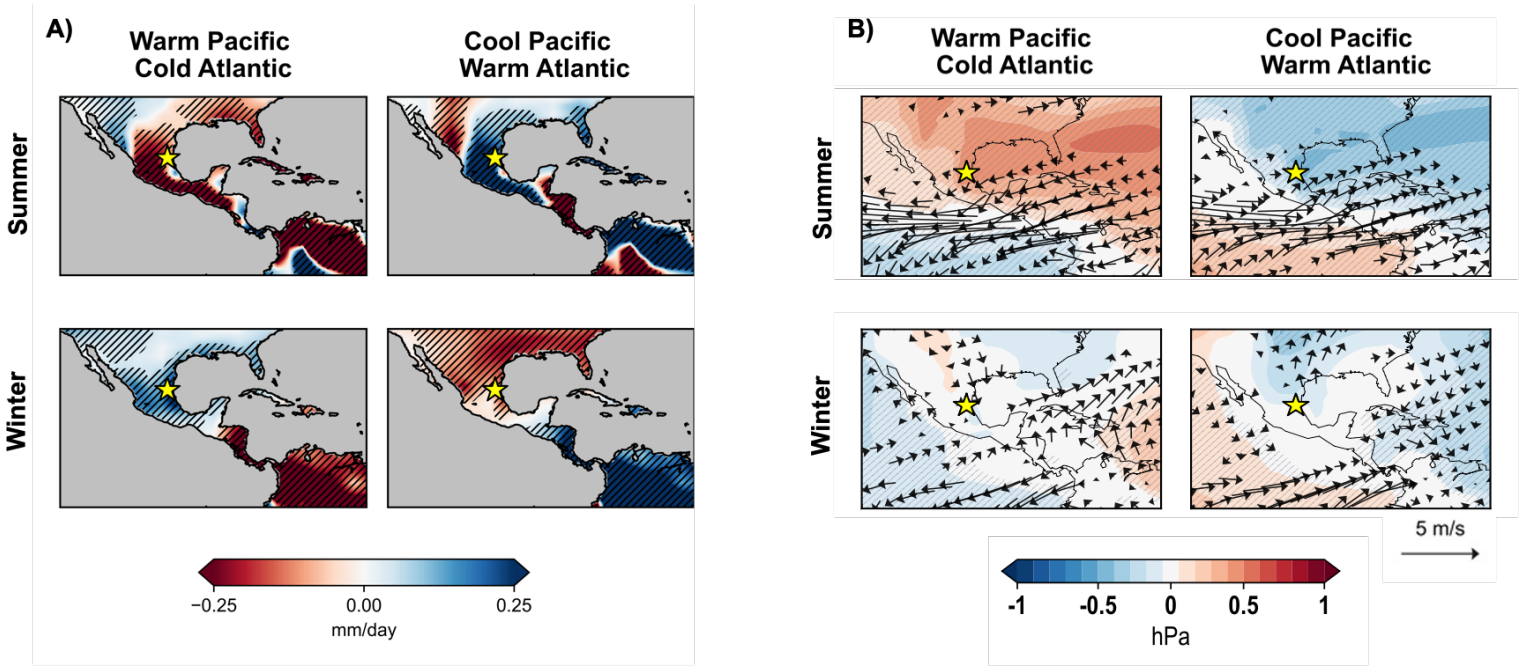

Figure 4. Precipitation, sea level pressure, and low-level winds in response to forced SSTs. A) Results of net precipitation change in the forced-SST simulations. Statistically significant changes (90% CI) are shaded by the hatching. B) Results of anomalous low-level wind patterns and sea level pressure (SLP) in response to forced SST simulations. Changes in SLPs are indicated by color, statistically significant changes are indicated by hatching. Only statistically significant low-level winds are plotted. Cueva Bonita indicated by the star.

have linked decreased vertical wind shear to more frequent and larger magnitude hurricanes in the Tropical North Atlantic.

Another notable result of the fixed SST simulations is the contrasting response of precipitation throughout most of Mexico during summer and winter (Figure 4, Figure S11). The only region that appears to respond consistently in both seasons is Northwest Mexico, which is strongly influenced by the North American Monsoon and is likely to be more sensitive to variability in Pacific SSTs. In response to a warm Pacific/cold Atlantic, winter precipitation throughout much of Mexico slightly increases. Increased winter precipitation in Northwest and Central Mexico has been attributed to a strengthening of North Pacific storm-track extending further south and west in response to anomalous Rossby waves (Seager & Hoerling, 2014). While this is not likely to drive increased precipitation in NE Mexico (Wright et al., 2021), anomalous northerly low-level winds could drive more frequent and intensified cold fronts from the North, increasing light, low-intensity rainfall to the region (Figure 4). This appears to be an important control of winter precipitation, as a reversal of the wind patterns under opposing SST conditions drives a reduction in regional precipitation. Winter simulations of rainfall support tree ring interpretations of 1) an out-of-phase dipole spatial pattern and 2) a dominant role of Pacific SSTs in controlling regional precipitation. However, winter precipitation only accounts for a small fraction of total annual rainfall, with winter contributing less than 7% of annual rainfall in NE Mexico. We therefore suggest relative changes in Atlantic SSTs are much more important in controlling precipitation in the region.

The new CB4 speleothem record from NE Mexico combined with forced-SST climate model results highlights the precipitation dipole pattern is far more spatially complex in Mexico than previously thought (Figure S13-14). We suggest previous reconstructions of the dipole pattern may have utilized tree rings and lake level records that are potentially biased towards winter, spring or early-summer rainfall (Stahle et al., 2016, 2020), minimizing the role of the Atlantic in modulating late-summer and early-autumn precipitation throughout most of the region. While variability in Pacific SSTs can still play a secondary role in regulating precipitation, mainly by controlling the amount of winter precipitation and summer vertical wind shear in the Tropical North Atlantic, we suggest this has the opposite effect on NE Mexico rainfall than previously thought. We suggest warmer Pacific SSTs predominantly drive decreased precipitation over the region.

4 Conclusions

Anthropogenic carbon emissions will continue to warm Tropical Atlantic SSTs in the future (Chen et al., 2018). Given the observed trend of increased precipitation in NE Mexico over the industrial period, this may suggest NE Mexico will become wetter, contrasting current model predictions. Importantly, however, forced-SST experiments elucidate precipitation in Mexico is most sensitive to the relative warming of the Tropical Atlantic, in comparison to the Tropical Pacific. Current model predictions of Tropical SSTs range significantly and exhibit significant bias, particularly in the Atlantic (Imbol Nkwinkwa et al., 2021). Improving model projections of Tropical SSTs is therefore crucial to predicting precipitation in the water stressed regions of Mexico and Central America, as shown by the sensitivity of rainfall to the relative warming of the Atlantic in our record.

Acknowledgments

We thank Cheva Berrones-Benitez for her assistance with rainfall sampling. We thank Jim Kennedy, Esteban Berrones, Corinne Wong, and Chris Wood for their help with fieldwork. We thank Dachun Zhang, Jessica Wang, Chris Wood, and Elizabeth Patterson for assistance with lab work. We thank Crystal Tulley-Cordova for sharing the precipitation collector design. This research was supported by a UC MEXUS-CONACYT Collaborative Grant from the University of California Institute for Mexico and the United States (UC MEXUS CN-16-120), an MIT International Science and Technology Initiatives Mexico Program, and National Science Foundation awards AGS-1804512 and AGS-1806090. K.R.J., D.M., K.T.W., and L.B-O. designed the study; K.T.W., G.S.M, K.R.J., and J-L.L.M. conducted fieldwork; K.T.W., G.S.M., G.R.G., and G.L. conducted laboratory analyses; C.R.T conducted paleoclimate model simulations; T.B., C.R.T., and K.T.W. analyzed model data; K.T.W. and K.R.J wrote the manuscript with help from coauthors. All authors contributed to data analysis and interpretation. The authors report no competing interests.

Open Research

Speleothem stable isotope, trace element and dead carbon proportion data utilized to reconstruct precipitation from CB4 is included in a SI file (CB4 data). Radiocarbon and U-Th results are included in Tables in SI (Supplementary Material). Authors further plan to add speleothem data to the NOAA Paleoclimate database once published. Version 1.15 of the COPRA depth-age modeling software utilized to build the age model in this study is available at [doi:10.5194/cp-8-1765-2012].

References

Asmerom, Y., Baldini, J. U. L., Prufer, K. M., Polyak, V. J., Ridley, H. E., Aquino, V. V, et al. (2020). Intertropical convergence zone variability in the Neotropics during the Common Era. *Science Advances*, *6*(7), 3644–3658. https://doi.org/10.1126/sciadv.aax3644

Bajo, P., Borsato, A., Drysdale, R., Hua, Q., Frisia, S., Zanchetta, G., et al. (2017). Stalagmite carbon isotopes and dead carbon proportion (DCP) in a near-closed-system situation: An interplay between sulphuric and carbonic acid dissolution. *Geochimica et Cosmochimica Acta*, *210*, 208–227. https://doi.org/10.1016/j.gca.2017.04.038

Baker, A., Berthelin, R., Cuthbert, M. O., Treble, P. C., Hartmann, A., & KSS Cave Studies Team, T. (2020). Rainfall recharge thresholds in a subtropical climate determined using a regional cave drip water monitoring network. *Journal of Hydrology*, *587*, 125001. https://doi.org/10.1016/j.jhydrol.2020.125001

Beverly, R. K., Beaumont, W., Tauz, D., Ormsby, K. M., von Reden, K. F., Santos, G. M., & Southon, J. R. (2010). The keck carbon cycle ams laboratory, university of california, irvine: Status report. *Radiocarbon*, *52*(2), 301–309. https://doi.org/10.1017/S0033822200045343

Bhatia, K. T., Vecchi, G. A., Knutson, T. R., Murakami, H., Kossin, J., Dixon, K. W., & Whitlock, C. E. (2019). Recent increases in tropical cyclone intensification rates. *Nature Communications*, *10*(1), 1–9. https://doi.org/10.1038/s41467-019-08471-z

Bhattacharya, T., & Coats, S. (2020). Atlantic-Pacific Gradients Drive Last Millennium Hydroclimate Variability in Mesoamerica. *Geophysical Research Letters*, *47*(13), e2020GL088061. https://doi.org/10.1029/2020GL088061

Bhattacharya, T., Chiang, J. C. H., & Cheng, W. (2017). Ocean-atmosphere dynamics linked to 800–1050 CE drying in mesoamerica. *Quaternary Science Reviews*, *169*, 263–277. https://doi.org/10.1016/j.quascirev.2017.06.005

Borsato, A., Johnston, V. E., Frisia, S., Miorandi, R., Corradini, F., Au, (A, & Borsato,). (2016). Temperature and altitudinal influence on karst dripwater chemistry: Implications for regional-scale palaeoclimate reconstructions from speleothems Cosmogenic Cl-36 in speleothems as a potential solar proxy View project OLOAMBIENT View project Temperature and altitudinal influence on karst dripwater chemistry: Implications for regional-scale palaeoclimate reconstructions from speleothems. *Geochimica et Cosmochimica Acta*, *177*, 275–297. https://doi.org/10.1016/j.gca.2015.11.043

Breitenbach, S. F. M., Rehfeld, K., Goswami, B., Baldini, J. U. L., Ridley, H. E., Kennett, D. J., et al. (2012). Constructing proxy records from age models (COPRA). *Climate of the Past*, *8*(5), 1765–1779. https://doi.org/10.5194/cp-8-1765-2012

Burns, S. J., Godfrey, L. R., Faina, P., Mcgee, D., Hardt, B., Ranivoharimanana, L., & Randrianasy, J. (2016). Rapid human-induced landscape transformation in Madagascar at the end of the first millennium of the Common Era. https://doi.org/10.1016/j.quascirev.2016.01.007

Chen, Y., Langenbrunner, B., & Randerson, J. T. (2018). Future Drying in Central America and Northern South America Linked With Atlantic Meridional Overturning Circulation. *Geophysical Research Letters*, *45*(17), 9226–9235. https://doi.org/10.1029/2018GL077953

Chiang, J. C. H., & Sobel, A. H. (2002). Tropical tropospheric temperature variations caused by ENSO and their influence on the remote tropical climate. *Journal of Climate*, *15*(18), 2616–2631. https://doi.org/10.1175/1520-0442(2002)015<2616:TTTVCB>2.0.CO;2

Curtis, S. (2008). The Atlantic multidecadal oscillation and extreme daily precipitation over the US and Mexico during the hurricane season. *Climate Dynamics*, *30*(4), 343–351. https://doi.org/10.1007/s00382-007-0295-0

Fohlmeister, J., Kromer, B., & Mangini, A. (2011). The influence of soil organic matter age spectrum on the reconstruction of atmospheric 14C levels via stalagmites. *Radiocarbon*, *53*(1), 99–115. https://doi.org/10.1017/S003382220003438X

Ford, D. C. (2000). Deep phreatic caves and groundwater systems of the Sierra de El Abra, Mexico. *Speleogenesis: Evolution of Karst Aquifers: Huntsville, Alabama, National Speleological*, 325–331.

Fosu, B., He, J., & Liguori, G. (2020). Equatorial Pacific Warming Attenuated by SST Warming Patterns in the Tropical Atlantic and Indian Oceans. *Geophysical Research Letters*, *47*(18), e2020GL088231. https://doi.org/10.1029/2020GL088231

Frisia, S., Fairchild, I. J., Fohlmeister, J., Miorandi, R., Spötl, C., & Borsato, A. (2011). Carbon mass-balance modelling and carbon isotope exchange processes in dynamic caves. *Geochimica et Cosmochimica Acta*, *75*(2), 380–400. https://doi.org/10.1016/J.GCA.2010.10.021

Gary, M. S. J. (2006). Volcanogenic karstification of Sistema Zacatón, Mexico, 79–89. https://doi.org/10.1130/2006.2404(08)

Genty, D., & Massault, M. (1997). Bomb14C recorded in laminated speleothems: Calculation of dead carbon proportion. *Radiocarbon*, *39*(1), 33–48. https://doi.org/10.1017/S0033822200040881

Genty, D., Massault, M., Gilmour, M., Baker, A., Verheyden, S., & Kepens, E. (1999). Calculation of past dead carbon proportion and variability by the comparison of AMS 14C and TIMS U/Th ages on two Holocene stalagmites. *Radiocarbon*, *41*(3), 251–270. https://doi.org/10.1017/S003382220005712X

St. George, S., Meko, D. M., & Cook, E. R. (2010). The seasonality of precipitation signals embedded within the North American Drought Atlas. *Holocene*, *20*(6), 983–988. https://doi.org/10.1177/0959683610365937

Giannini, A., Kushnir, Y., & Cane, M. A. (2000). Interannual variability of Caribbean rainfall, ENSO, and the Atlantic Ocean. *Journal of Climate*, *13*(2), 297–311. https://doi.org/10.1175/1520-0442(2000)013<0297:IVOCRE>2.0.CO;2

Giannini, A., Chiang, J. C. H., Cane, M. A., Kushnir, Y., & Seager, R. (2001). The ENSO teleconnection to the Tropical Atlantic Ocean: Contributions of the remote and local SSTs to rainfall variability in the Tropical Americas. *Journal of Climate*, *14*(24), 4530–4544. https://doi.org/10.1175/1520-0442(2001)014<4530:TETTTT>2.0.CO;2

Gram, W. K., & Faaborg, J. (1997). The Distribution of Neotropical Migrant Birds Wintering in the El Cielo Biosphere Reserve, Tamaulipas, Mexico. *The Condor*, *99*(3), 658–670. https://doi.org/10.2307/1370478

Gray, S. T., Graumlich, L. J., Betancourt, J. L., & Pederson, G. T. (2004). A tree-ring based reconstruction of the Atlantic Multidecadal Oscillation since 1567 A.D. *Geophysical Research Letters*, *31*(12), n/a-n/a. https://doi.org/10.1029/2004GL019932

Griffiths, M. L., Fohlmeister, J., Drysdale, R. N., Hua, Q., Johnson, K. R., Hellstrom, J. C., et al. (2012). Hydrological control of the dead carbon fraction in a Holocene tropical speleothem. *Quaternary Geochronology*, *14*, 81–93. https://doi.org/10.1016/j.quageo.2012.04.001

Griffiths, M. L., Johnson, K. R., Pausata, F. S. R., White, J. C., Henderson, G. M., Wood, C. T., et al. (2020). End of Green Sahara amplified mid- to late Holocene megadroughts in mainland Southeast Asia. *Nature Communications*, *11*(1), 4204. https://doi.org/10.1038/s41467-020-17927-6

Gutiérrez-García, G., Beramendi-Orosco, L. E., & Johnson, K. R. (2020). Climate-growth relationships of Pinus pseudostrobus from a tropical mountain cloud forest in northeast Mexico. *Dendrochronologia*, *64*, 125749. https://doi.org/10.1016/j.dendro.2020.125749

Hammer, Ø., Harper, D. A. T., & Ryan, P. D. (2001). Past: Paleontological statistics software package for education

442 and data analysis. *Palaeontologia Electronica*, *4*(1), 178. Retrieved from http://palaeo-
443 electronica.orghttp//palaeo-electronica.org/2001_1/past/issue1_01.htm.
444 He, J., & Soden, B. J. (2017). A re-examination of the projected subtropical precipitation decline. *Nature Climate*
445 *Change*, *7*(1), 53–57. https://doi.org/10.1038/nclimate3157
446 Hendy, C. H. (1971). The isotopic geochemistry of speleothems-I. The calculation of the effects of different modes
447 of formation on the isotopic composition of speleothems and their applicability as palaeoclimatic indicators.
448 *Geochimica et Cosmochimica Acta*, *35*(8), 801–824. https://doi.org/10.1016/0016-7037(71)90127-X
449 Hidalgo, H. G., Amador, J. A., Alfaro, E. J., & Quesada, B. (2013). Hydrological climate change projections for
450 Central America. *Journal of Hydrology*, *495*, 94–112. https://doi.org/10.1016/j.jhydrol.2013.05.004
451 Imbol Nkwinkwa, A. S. N., Latif, M., & Park, W. (2021). Mean-State Dependence of CO 2 -Forced Tropical
452 Atlantic Sector Climate Change. *Geophysical Research Letters*, *48*(19), e2021GL093803.
453 https://doi.org/10.1029/2021gl093803
454 Johnson, K. R., Hu, C., Belshaw, N. S., & Henderson, G. M. (2006). Seasonal trace-element and stable-isotope
455 variations in a Chinese speleothem: The potential for high-resolution paleomonsoon reconstruction. *Earth and*
456 *Planetary Science Letters*, *244*(1–2), 394–407. https://doi.org/10.1016/j.epsl.2006.01.064
457 Kovaltsov, G. A., Mishev, A., & Usoskin, I. G. (2012). A new model of cosmogenic production of radiocarbon 14C
458 in the atmosphere. *Earth and Planetary Science Letters*, *337–338*, 114–120.
459 https://doi.org/10.1016/j.epsl.2012.05.036
460 Lachniet, M. S., Burns, S. J., Piperno, D. R., Asmerom, Y., Polyak, V. J., Moy, C. M., & Christenson, K. (2004). A
461 1500-year El Niño/Southern Oscillation and rainfall history for the Isthmus of Panama from speleothem
462 calcite. *Journal of Geophysical Research D: Atmospheres*, *109*(20), 20117.
463 https://doi.org/10.1029/2004JD004694
464 Lachniet, M. S., Asmerom, Y., Polyak, V., & Bernal, J. P. (2017). Two millennia of Mesoamerican monsoon
465 variability driven by Pacific and Atlantic synergistic forcing. *Quaternary Science Reviews*, *155*, 100–113.
466 https://doi.org/10.1016/j.quascirev.2016.11.012
467 Lawrence Edwards, R., Chen, J. H., & Wasserburg, G. J. (1987). 238U234U230Th232Th systematics and the
468 precise measurement of time over the past 500,000 years. *Earth and Planetary Science Letters*, *81*(2–3), 175–
469 192. https://doi.org/10.1016/0012-821X(87)90154-3
470 Li, L., & Chakraborty, P. (2020). Slower decay of landfalling hurricanes in a warming world. *Nature*, *587*(7833),
471 230–234. https://doi.org/10.1038/s41586-020-2867-7
472 Marsh, D. R., Mills, M. J., Kinnison, D. E., Lamarque, J. F., Calvo, N., & Polvani, L. M. (2013). Climate change
473 from 1850 to 2005 simulated in CESM1(WACCM). *Journal of Climate*, *26*(19), 7372–7391.
474 https://doi.org/10.1175/JCLI-D-12-00558.1
475 Martín-Chivelet, J., Belén Muñoz-García, M., Cruz, J. A., Ortega, A. I., Turrero, M. J., & Jones, B. (2017).
476 Speleothem Architectural Analysis: Integrated approach for stalagmite-based paleoclimate research.
477 https://doi.org/10.1016/j.sedgeo.2017.03.003
478 Martinez-Lopez, B., Quintanar, A. I., Cabos-Narvaez, W. D., Gay-Garcia, C., & Sein, D. V. (2018). Nonlinear
479 Trends and Nonstationary Oscillations as Extracted From Annual Accumulated Precipitation at Mexico City.
480 *Earth and Space Science*, *5*(9), 473–485. https://doi.org/10.1029/2018EA000395
481 McCabe-Glynn, S., Johnson, K. R., Strong, C., Berkelhammer, M., Sinha, A., Cheng, H., & Edwards, R. L. (2013).
482 Variable North Pacific influence on drought in southwestern North America since AD 854. *Nature*
483 *Geoscience*, *6*(8), 617–621. https://doi.org/10.1038/ngeo1862
484 Noronha, A. L., Johnson, K. R., Southon, J. R., Hu, C., Ruan, J., & McCabe-Glynn, S. (2015). Radiocarbon
485 evidence for decomposition of aged organic matter in the vadose zone as the main source of speleothem
486 carbon. *Quaternary Science Reviews*, *127*, 37–47. https://doi.org/10.1016/J.QUASCIREV.2015.05.021
487 Rayner, N. A., Parker, D. E., Horton, E. B., Folland, C. K., Alexander, L. V, Rowell, D. P., et al. (2003). Global
488 analyses of sea surface temperature, sea ice, and night marine air temperature since the late nineteenth century.
489 *Journal of Geophysical Research: Atmospheres*, *108*(14), 4407. https://doi.org/10.1029/2002jd002670
490 Reimer, P. J., Bard, E., Bayliss, A., Beck, J. W., Blackwell, P. G., Ramsey, C. B., et al. (2013). Selection and
491 Treatment of Data for Radiocarbon Calibration: An Update to the International Calibration (IntCal) Criteria.
492 *Radiocarbon*, *55*(4), 1923–1945. https://doi.org/10.2458/azu_js_rc.55.16955
493 Roy, P. D., Rivero-Navarrete, A., Sánchez-Zavala, J. L., Beramendi-Orosco, L. E., Muthu-Sankar, G., & Lozano-
494 Santacruz, R. (2016). Atlantic Ocean modulated hydroclimate of the subtropical northeastern Mexico since the
495 last glacial maximum and comparison with the southern US. *Earth and Planetary Science Letters*, *434*, 141–
496 150. https://doi.org/10.1016/j.epsl.2015.11.048
497 Roy, P. D., Vera-Vera, G., Sánchez-Zavala, J. L., Shanahan, T. M., Quiroz-Jiménez, J. D., Curtis, J. H., et al.

(2020). Depositional histories of vegetation and rainfall intensity in Sierra Madre Oriental Mountains (northeast Mexico) since the late Last Glacial. *Global and Planetary Change*, *187*(July 2019), 103136. https://doi.org/10.1016/j.gloplacha.2020.103136

Sachs, J. P., Sachse, D., Smittenberg, R. H., Zhang, Z., Battisti, D. S., & Golubic, S. (2009). Southward movement of the Pacific intertropical convergence zone AD 1400-1850. *Nature Geoscience*, *2*(7), 519–525. https://doi.org/10.1038/ngeo554

Sanders, W. T., Parsons, J. R., & Santley, R. S. (1979). The Basin of Mexico: Ecological Processes in the Evolution of a Civilization. *Academic Press*, 561.

Schlesinger, M. E., & Ramankutty, N. (1994). An oscillation in the global climate system of period 65-70 years. *Nature*, *367*(6465), 723–726. https://doi.org/10.1038/367723a0

Schulz, M., & Mudelsee, M. (2002). REDFIT: Estimating red-noise spectra directly from unevenly spaced paleoclimatic time series. *Computers and Geosciences*, *28*(3), 421–426. https://doi.org/10.1016/S0098-3004(01)00044-9

Seager, R., & Hoerling, M. (2014). Atmosphere and ocean origins of North American droughts. *Journal of Climate*, *27*(12), 4581–4606. https://doi.org/10.1175/JCLI-D-13-00329.1

Smith, K. L., Neely, R. R., Marsh, D. R., & Polvani, L. M. (2015). The Specified Chemistry Whole Atmosphere Community Climate Model (SC-WACCM). *Journal of Advances in Modeling Earth Systems*, *6*(3), 883–901. https://doi.org/10.1002/2014MS000346

Stahle, D. W., Cook, E. R., Burnette, D. J., Villanueva, J., Cerano, J., Burns, J. N., et al. (2016, October 1). The Mexican Drought Atlas: Tree-ring reconstructions of the soil moisture balance during the late pre-Hispanic, colonial, and modern eras. *Quaternary Science Reviews*. Pergamon. https://doi.org/10.1016/j.quascirev.2016.06.018

Stahle, D. W., Cook, E. R., Burnette, D. J., Torbenson, M. C. A., Howard, I. M., Griffin, D., et al. (2020). Dynamics, Variability, and Change in Seasonal Precipitation Reconstructions for North America. *Journal of Climate*, *33*(8), 3173–3195. https://doi.org/10.1175/JCLI-D-19-0270.1

Villanueva-Diaz, J., Stahle, D. W., Luckman, B. H., Cerano-Paredes, J., Therrell, M. D., Cleaveland, M. K., et al. (2007). Winter-spring precipitation reconstructions from tree rings for northeast Mexico the Tropical Rainfall Index) indicated long-term instability of the Pacific equa-torial teleconnection. Atmospheric circulation systems coming from higher latitudes (cold. *Climatic Change*, *83*, 117–131. https://doi.org/10.1007/s10584-006-9144-0

Wang, C. (2007). Variability of the Caribbean Low-Level Jet and its relations to climate. *Climate Dynamics*, *29*(4), 411–422. https://doi.org/10.1007/s00382-007-0243-z

Wang, C., & Lee, S. K. (2007). Atlantic warm pool, Caribbean low-level jet, and their potential impact on Atlantic hurricanes. *Geophysical Research Letters*, *34*(2), L02703. https://doi.org/10.1029/2006GL028579

Wogau, K. H., Arz, H. W., Böhnel, H. N., Nowaczyk, N. R., & Jungjae, P. (2019). High resolution paleoclimate and paleoenvironmental reconstruction in the Northern Mesoamerican Frontier for Prehistory to Historical times. *Quaternary Science Reviews*, *226*, 106001. https://doi.org/10.1016/j.quascirev.2019.106001

Wright, K., Johnson, K., Marks, G. S., Mcgee, D., Goldsmith, G. R., Tabor, C., et al. (2021). Thermodynamics control precipitation in NE Mexico on orbital to millennial timescales, 0–25. https://doi.org/10.21203/RS.3.RS-611282/V1